High Magnetic Field Sensor Using LaSb₂

D.P. Young, R.G. Goodrich, J.F. DiTusa, S. Guo, and P.W. Adams

Department of Physics and Astronomy

Louisiana State University

Baton Rouge, Louisiana, 70803

Julia Y. Chan Department of Chemistry Louisiana State University Baton Rouge, LA, 70803

Donavan Hall*
National High Magnetic Field Laboratory
Florida State University
Tallahassee, FL, 32306
(Dated: September 6, 2018)

The magnetotransport properties of single crystals of the highly anisotropic layered metal LaSb₂ are reported in magnetic fields up to 45 T with fields oriented both parallel and perpendicular to the layers. Below 10 K the perpendicular magnetoresistance of LaSb₂ becomes temperature independent and is characterized by a 100-fold linear increase in resistance between 0 and 45 T with no evidence of quantum oscillations down to 50 mK. The Hall resistivity is hole-like and gives a high field carrier density of $n \sim 3 \times 10^{20}$ cm⁻³. The feasibility of using LaSb₂ for magnetic field sensors is discussed.

One of the most successful strategies for producing technologically relevant magnetoresistive materials is to enhance the effects of field-dependent magnetic scattering processes through the creation of magnetic superlattices [1] or by doping magnetic insulators such that a magnetic and metal-insulator transition coincide [2]. Unexpectedly, there have been several recent discoveries of a large, non-saturating magnetoresistance (MR) in low carrier density non-magnetic metals [3, 4, 5, 6, 7] and semiconductors [8]. One class of these systems, the slightly off-stoichiometric silver chalcogenides, $Ag_{2+\delta}Te$ and $Ag_{2+\delta}Se$, have shown significant promise as the basis of ultra-high magnetic field sensors by virtue of the fact that they exhibit a multi-fold, quasi-linear MR that remains unsaturated up to 60 T [8]. In this Letter we present magnetotransport data on the highly layered non-magnetic metal LaSb₂ which displays a 100-fold, linear MR with no sign of saturation up to 45 T. We show that in many respects, including sensitivity, linearity, synthesis characteristics and intrinsic anisotropy, LaSb₂ is a compelling candidate for high-field sensor development.

LaSb₂ is a member of the RSb₂ (R=La-Nd, Sm) family of compounds that all form in the orthorhombic SmSb₂ structure [9, 10]. LaSb₂, in particular, is comprised of alternating La/Sb layers and two-dimensional rectangular sheets of Sb atoms stacked along the c-axis [11]. Similar structural characteristics give rise to the anisotropic physical properties observed in all the compounds in the RSb₂ series [12]. Since LaSb₂ is non-magnetic, its low-temperature transport properties are not complicated by magnetic phase transitions which occur in the other members of this series [12].

Single crystals of LaSb₂ were grown from high purity La and Sb by the metallic flux method [13]. The orthorhombic SmSb₂-structure type was confirmed by single crystal X-ray diffraction. The crystals grow as large flat layered plates which are malleable and easily cleaved. Typically flux grown samples had dimensions of 5mm x 5mm x 0.2mm. Electrical contact was made using Epotek [14] silver epoxy and 1 mil gold wire. Transport properties were measured using a 27 Hz 4-probe AC technique at temperatures from 0.03 - 300 K and in magnetic fields up to 45 T. In all of the measurements presented probe currents of 1 - 5 mA where used with corresponding power levels less than 10 nW. Hall effect measurements were made on natural thickness samples in a 4-wire geometry with data being taken in both positive and negative fields up to 30 T.

The in-plane zero-field electrical resistivity, ρ , of single crystals of LaSb₂ was measured from 1.8-300 K and found to be metallic $(d\rho/dT > 0)$. The residual resistivity ratio (RRR) was large $(\rho_{ab}(300K)/\rho_{ab}(2K) \approx 70-90)$, indicating a high sample quality. In the main panel of Fig. 1 we show the transverse MR with the field oriented parallel and perpendicular to the ab-plane. Both MR's are positive and nearly linear above 2 T. Note the extreme anisotropy in the magnetotransport with the perpendicular MR being an order of magnitude larger than the parallel MR. The perpendicular MR was large, with resistance increasing by a factor of 90 from 0 to 45 T. The MR was temperature

^{*}Present address: American Physical Society, One Research Road, Box 9000, Ridge, NY 11961

independent below 10 K but decreased rapidly above 30 K. Interestingly, there is no evidence of saturation or quantum oscillations in the MR of Fig. 1 which has obvious advantages for magnetic field sensor applications. The solid lines in Fig. 1 are least-square fits to a fourth-order polynomial (Table 1). Note the high quality of the fits to the MR using this simple functional form. The relative field sensitivity, which is the figure of merit for a sensor, is represented by $\alpha_1 = 1.23 \text{ T}^{-1}$. This sensitivity is roughly a factor of 4 greater than that of $Ag_{2+\delta}Se$ (triangle symbols in Fig. 1).

The anisotropy of the MR can be demonstrated by measuring the transverse MR as a function of the tilt angle in a constant magnetic field. In Fig. 2 we plot the resistivity normalized by the parallel field value, $\rho(H_{\perp}=0)$, as a function of the perpendicular component of the field H_{\perp} . Interestingly, the general shape of the MR curves in Fig. 2 is quite similar to those of Fig. 1. The solid lines are polynomial fits to the data (Table 1). In terms of a magnetic field sensor, this anisotropy can be exploited to determine the angle of orientation in tilted field studies. The micaceous nature of LaSb₂ not only produces an anisotropic MR but also presents a convenient geometry for Hall measurements, namely large flat crystals. In the main panel of Fig. 3 we plot the Hall resistivity, ρ_{xy} , as a function of magnetic field at T = 2 K. In the right inset of Fig. 3 we show the low field behavior of ρ_{xy} which is negative below 0.5 T but becomes positive at higher fields. This latter behavior is often characteristic of a two-carrier system [18]. In the high field limit the majority carrier dominates, which in our case is hole-like. Above 10 T the Hall constant is $R_H \sim 2 \times 10^{-6} \ \mu\Omega$ -cm/T which corresponds to a carrier density of n $\sim 3 \times 10^{20}$ cm⁻³ and a Hall mobility $\mu \sim 0.05$ m²/Vs. We note that the overall shape of the Hall resistance curve in the right inset of Fig. 3, with its local minimum, is very similar in character to that of NbSe₂ and TaSe₂ which also form in non-magnetic micaceous crystalline structures [15].

A useful measure of the magnitude of the linear MR is the dimensionless Kohler slope, $S = (1/R_H)(d\rho(H)/dH)$. Combining the Hall constant measurements with the value of α_1 , obtained from the MR of Fig. 1, we get a high field value $S \sim 0.6$. This value is an order of magnitude larger than what is typical of other non-magnetic systems displaying a linear MR. Classically, the MR should vary quadratically with field. In a closed orbit system the MR saturates in the high field limit limit, $\omega_c \tau \gg 1$, where ω_c is the cyclotron frequency and τ is the elastic scattering time [18]. Over the past 30 years several mechanisms have been proposed to account for anomalous linear MR observed in a wide variety non-magnetic systems such as elemental metals [5, 19], two-dimensional heterostructures [20], and disordered semiconductors [8]. Theories accounting for linear MR fall into two main categories. The first contains theories associated with the alteration of the structural symmetry due to the formation of a charge density wave (CDW) [21]. Linear MR in very pure elemental metals has been attributed to quantum fluctuations about a CDW ground state [16] and/or a magnetic breakdown of the CDW gap [15, 17]. The second includes theories which invoke high field quantization effects or singular scattering mechanisms which cannot be accounted for by the standard perturbative scattering formulations [3, 22]. Interestingly, the transition metal dichalogenides NbSe₂ and TaSe₂ both have well established CDW ground states and exhibit an anomalous linear MR. These compounds are similar in structure to LaSb₂, suggesting that perhaps a CDW state plays a central role in the MR of LaSb₂. At this time, however, is not known whether LaSb₂ undergoes a charged density wave transition.

It has been known for many years that the relative MR, $\Delta \rho/\rho$, of many metals and semimetals is a temperature independent function of magnetic field [23]. In particular, $\Delta \rho/\rho = F(H)$, where F(H) usually has a power-law form. LaSb₂ is known to obey this rule, commonly referred to as Kohler's rule, with $F(H) \sim H$ [12]. One can also make a similar analysis by substituting the Hall resistance for the magnetic field H. The resulting modified Kohler plot for LaSb₂ is shown in the left inset of Fig. 3. The solid line in the plot has a slope of $\nu = 2/3$ indicating that $\Delta \rho \propto \rho_{xy}^{2/3}$. Interesingly, Ag_{2+ δ}Se also exhibits power-law behavior but with a low temperature modified Kohler slope of $\nu = 5/3$ [8]. This suggests that the underlying MR mechanisms in these two seemingly unrelated systems may be similar and that the differing scaling exponents is a dimensionality effect.

In conclusion, we show that crystalline LaSb₂ is an attractive material for use as a high magnetic field sensor. It is relatively easy to synthesize, and electrical contact can be made with silver epoxy. By virtue of its highly anisotropic structure, LaSb₂ can be used in either a transverse MR configuration or a Hall configuration. The sensitivity in both configurations is quite good. Calibration curves for both the MR and the Hall resistance can be made using a fourth-order polynomial, thus avoiding numerical difficulties associated with complicated fitting forms.

We gratefully acknowledge discussions with Dana Browne and Richard Kurtz. This work was supported by the National Science Foundation under Grants DMR 99-72151 and DMR 01-03892. We also acknowledge support of the Louisiana Education Quality Support Fund under Grant No. 2001-04-RD-A-11. A portion of this work was performed at the National High Magnetic Field Laboratory, which is supported by NSF Cooperative Agreement No. DMR-9527035 and by the State of Florida.

- M.N. Baibich, J.M Broto, A. Fert, F.N. Vandau, F. Petroff, P. Eitenne, G. Creuzet, A. Friederich, and J. Chazelas, Phys. Rev. Lett. 61, 2472 (1988); R.E. Camlery and R.L. Stamps, J. Phys. Cond. Matter 5, 3727 (1993).
- [2] S. Jin, T.H. Tiefel, M. McCormack M, R.A. Fastnacht, R. Ramesh, and L.H. Chen, Science 264, 413 (1994).
- [3] A.A. Abrikosov, Phys. Rev. B **60**, 4231 (1999); A.A. Abrikosov, Europhys. Lett., **49** (6), 789 (2000).
- [4] I.M. Lifshits and V.G. Peshanskii, Sov. Phys. JETP, 8, 875 (1959).
- L.M. Falicov and H. Smith, Phys. Rev. Lett. 29, 124 (1972).
- [6] D.E. Soule, Phys. Rev. 112, 698 (1958); J.W. McClure and W.J. Spry, Phys. Rev. 165, 809 (1968).
- [7] In this case a multi-fold positive, linear, magnetoconductance is seen, V.Yu. Butko, J.F. Ditusa, and P.W. Adams, Phys. Rev. Lett.85, 162 (2000); V.Yu. Butko and P.W. Adams, Nature 409, 161 (2001).
- [8] A. Husmann, J.B. Betts, G.S. Boebinger, A. Migliori, T.F. Rosenbaum, and L. Saboungi, Nature 417, 421 (2002).
- [9] R. Wang and H. Steinfink, Inorg. Chem. 6, 1685 (1967).
- [10] F. Hullinger, in *Handbook of Physics and Chemistry of Rare Earths*, edited by K.A. Gschneidner and L. Eyring (North-Holland, Amsterdam, 1979), Vol. 4, p. 153.
- [11] X-ray analysis determined the lattice constants to be 0.6319 nm, 0.6173 nm, and 1.857 nm for the a, b, and c crystallographic directions, respectively.
- [12] S.L. Bud'ko, P.C. Canfield, C.H. Mielke, and A.H. Lacerda, Phys. Rev. B 57,13624 (1998).
- [13] P.C. Canfield and Z. Fisk, Philos. Mag. B 65, 1117 (1992).
- [14] Epoxy Technology, 14 Fortune Dr., Billerica, MA, 01821 (www.epotek.com).
- [15] M. Naito and S. Tanaka, J. Phys. Soc. Jpn. 51, 228 (1982).
- [16] A.H.C. Neto, Phys. Rev. Lett. 86, 4382 (2001).
- [17] J.A. Wilson, F.J. DiSalvo, and S. Mahajan, Adv. Phys. 24, 117 (1975).
- [18] N.W. Ashcroft and N.D. Mermin, Solid State Physics (Saunders, New York, 1976).
- [19] P.L. Kapitza, Proc. R. Soc. London, Ser. A, 119, 358 (1928).
- [20] H.L. Stormer, K.W. West, L.N. Pfeiffer, and K.W. West, Solid State Comm., 84, 95 (1992).
- [21] A.W. Overhauser, Phys. Rev. B 3, 3173 (1971).
- [22] R.A. Young, Phys. Rev. 175, 813 (1968).
- [23] A.A. Abrikosov, Fundamentals of the Theory of Metals (North-Holland, Amsterdam, 1988).

Figures

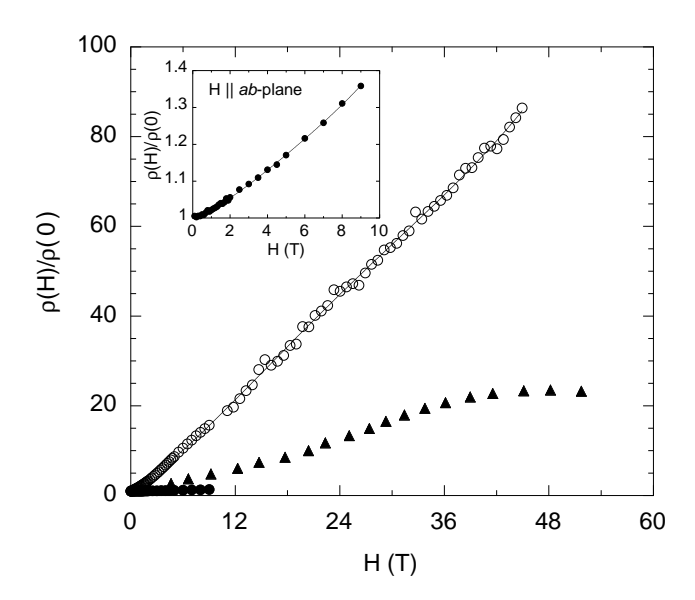


FIG. 1: Transverse MR of LaSb₂ at T=2 K with the current in the ab-plane and magnetic field oriented parallel (closed circles) and perpendicular (open circles) to the ab-plane. The solid triangles represent the MR of $Ag_{2+\delta}Se$ as taken from Ref. 8. Inset: Low field MR with H||ab-plane. The solid lines represent a least-squares fit to the data using a fourth-order polynomial (Table 1).

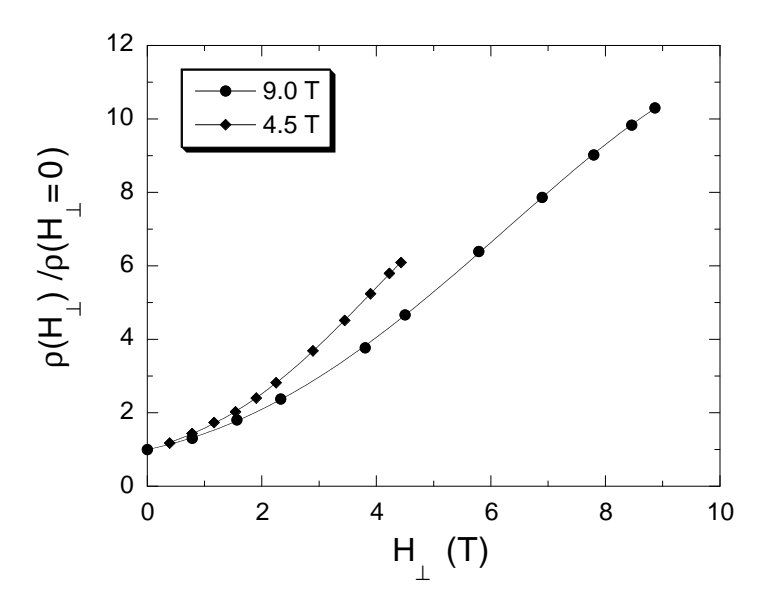


FIG. 2: MR in a tilted magnetic field. The samples were rotated out of the $H \parallel ab$ -plane in constant magnetic fields of 9.0 T and 4.5 T. The MR at 2 K is plotted as a function of the perpendicular component of the field. The solid lines represent a least-squares fit to the data using a fourth-order polynomial (Table 1).

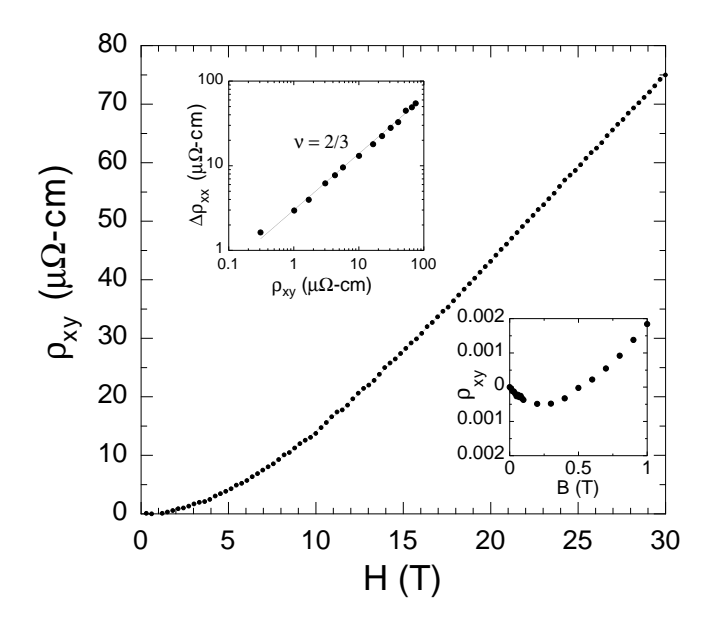


FIG. 3: Hall resistivity as a function of magnetic field at T = 2 K. The solid lines represent a least-squares fit to the data using a fourth-order polynomial (Table 1). Right inset: low field behavior of ρ_{xy} showing a crossover from electron-like to hole-like conduction with increasing field. Left inset: log-log plot of $\Delta \rho = \rho(H) - \rho(0)$ as a function of the Hall resistivity at T = 2 K. The solid line has slope $\nu = 2/3$. The linearity of the data suggests that $\Delta \rho \propto \rho_{xy}^{2/3}$.

Tables

TABLE I: Polynomial coefficients obtained from a least squares fit to the data in Figs. 1-3 using a fourth-order polynomial, $f(H) = \alpha_0 + \alpha_1 H + \alpha_2 H^2 + \alpha_3 H^2 + \alpha_4 H^4$.

| | α_0 | α_1 | α_2 | α_3 | α_4 |
|-------------------------------------------|------------|------------|--------------------------|---------------------------|--------------------------|
| $\rho(H)/\rho(0) (H \parallel \hat{c})$ | 1 | 1.236 | 0.0579 | -1.874×10^{-3} | $2.019 \text{x} 10^{-5}$ |
| $\rho(H)/\rho(0) \ (H \perp \hat{c})$ | 1 | 0.0182 | $5.601 \text{x} 10^{-3}$ | -6.260×10^{-4} | $3.032 \text{x} 10^{-5}$ |
| $\rho(H_{\perp})/\rho(0) \ (H = 9T)$ | 1 | 0.3315 | 0.1023 | 4.598×10^{-3} | -7.931×10^{-4} |
| $\rho(H_{\perp})/\rho(0) \ (H = 4.5T)$ | 1 | 0.4624 | 0.0827 | 0.04644 | -6.775×10^{-3} |
| $\rho_{xy}(H) \; (\mu \Omega \text{-cm})$ | 0 | 0.0225 | 0.1781 | $-4.309 \text{x} 10^{-3}$ | $3.757 \text{x} 10^{-5}$ |